

# An investigation on structure and characteristics of alpaca based wet-spun polyacrylonitrile composite fibres by utilizing natural textile waste

Md Abdullah Al Faruque, Rechana Remadevi, Joselito Razal, Xungai Wang and Maryam Naebe\*

*Deakin University, Institute for Frontier Materials (IFM), Geelong, Victoria 3216, Australia*

\*Corresponding author: maryam.naebe@deakin.edu.au

## **Abstract**

The composite alpaca/acrylic fibres were auspiciously produced through a wet spinning technique to reduce the consumption of petroleum-based polyacrylonitrile (PAN) and to enhance the thermal stability and moisture properties of the fibres. The waste alpaca fibres were converted into powder using a mechanical milling method without applying any chemicals. Alpaca powders were then blended with the polyacrylonitrile (PAN) dope solution in different weight ratios of alpaca: PAN (10:90, 20:80, and 30:70) to wet spin the composite fibres. The Fourier Transform Infrared (FTIR) spectroscopy showed that all the composite fibres possess the functional groups of both alpaca and PAN. The Nuclear Magnetic Resonance ( $^{13}\text{C}$  NMR) spectroscopy confirmed the presence of typical carbonyl carbon ( $\text{C}=\text{O}$ ) and nitrile carbon ( $\text{C}\equiv\text{N}$ ) peaks of protein and PAN, respectively. The Differential Scanning Calorimetry (DSC) and Thermogravimetric analysis (TGA) revealed the enhanced thermal stability of alpaca/PAN composite fibres. The moisture properties of the composite fibres were subsequently found to increase with the incorporation of alpaca, more than three times that of pure PAN fibres. These results revealed a potential green pathway to producing composite acrylic fibres with improved thermal and moisture properties by applying textile waste materials.

## 1. Introduction

The textile industry is one of the oldest industries in the world, which is not only fulfilling the demand for clothing but also the trend in the latest fashion <sup>1,2</sup>. The use of both natural and synthetic fibres is enormous in fulfilling this demand. In recent years, the production of polymeric synthetic fibres has increased rapidly, because these fibres can be tailored to the desired size, shape and properties <sup>3</sup>. Nowadays the application of fibres is not only limited to traditional apparel manufacturing but also used in energy storage, developing composite materials for reinforcement as well as functional fibres and fabrics <sup>4-7</sup>. These synthetic fibres application areas were found either by altering or by incorporating other functional materials into their polymeric chain. For example, it has been reported that the fibrils from polyethylene terephthalate (PET) have been successfully embedded into the polymeric matrix of polypropylene (PP) by adopting the fibre spinning process, to increase the mechanical properties and foaming ability of the polypropylene (PP) fibres <sup>8</sup>. Continuous bi-component melt spun polymer optical fibres (POFs) has been reported where cyclo-olefin polymer (COP) and tetrafluoroethylene-hexafluoropropylene-vinylidene fluoride terpolymer (THV) were used in the core and sheath, respectively to be used as sensors to determine the heart rate and oxygen saturation values of a human being <sup>9</sup>. However, the extensive use of synthetic fibres is not free from adverse environmental impact due to their petrochemical-based origin, non-biodegradable nature and use of various environmentally hazardous chemicals during production <sup>7</sup>.

After nylon and polyester, polyacrylonitrile (acrylic) is the third most widely used synthetic fibre which is synthesized from petrochemical sources <sup>10,11</sup>. Since production in the 1950s, acrylic has found tremendous application in clothing, industrial textiles, home textiles and in other technical textile fields due to their versatile characteristics <sup>11</sup>. In addition, it is extensively used as a precursor for the production of high strength carbon fibres <sup>10,12,13</sup>. However, higher

flammability, lower thermal stability, and moisture properties limit its further application in textile fields <sup>11,12</sup>. Generally, acrylic fibres are produced with at least 85% acrylonitrile monomer and the remaining 15% made up of different co-monomers based on textile end-use application <sup>10</sup>. Acrylic fibres are mainly produced by a solution spinning process (either wet spinning or dry spinning), not melt spinning. This is due to the degradation of the acrylonitrile polymer before reaching to its melting point <sup>10,11</sup>. Different organic solvent, for example, dimethylformamide (DMF), dimethylacetamide (DMAc) and dimethyl sulfoxide (DMSO) is used as a solvent to produce the acrylic fibres <sup>14</sup>. However, among these organic solvents, DMSO is less hazardous. In wet spinning, the PAN polymers are dissolved in the solvent and then passed through the coagulation process where fibre forms due to the counter-diffusion mechanism between the solvent and non-solvent (water) system <sup>15</sup>. The coagulation bath should consist of a mixture of solvent and non-solvent, as the higher solvent ratio can re-dissolve the fibres while higher non-solvent (water) content can produce fibres with larger voids that lead to fibres with low mechanical properties <sup>16,17</sup>.

It has already been reported that the production of acrylic fibres is possible with several physical and chemical modifications for various end uses <sup>18,19</sup>. Nevertheless, applying chemicals to modify the fibre properties is not free of environmental pollutions and impact on public health <sup>18,20</sup>. For example, different types of hazardous and toxic chemicals, consisting of halogen, phosphorus or sulphur are used to increase the flame retardant property of the PAN fibres <sup>21</sup>. Therefore, it is high time to follow the eco-friendly as well as a sustainable approach to boost the thermal stability, moisture absorption and non-flammability of acrylic fibres for different applications. Recently, a term “green-composite” or “bio-composite” has been developed where mainly cellulose-based natural fibres like cotton, hemp, and jute were mixed or blended with the synthetic materials to produce partially or completely biodegradable composite materials <sup>22-24</sup>. However, the application of natural protein fibres was not reported

to produce these types of composites. Additionally, enhancing the flame retardancy of the fibres by increasing the thermal stability while not applying any chemicals was overlooked in the works of literature.

Alpaca fibre is an expensive and luxurious animal fibre with a protein structure similar to wool and with excellent softness, warmth, strength and moisture properties <sup>25</sup>. In addition, being keratinous protein, inherently these fibres are biocompatible, biodegradable and fire-resistant <sup>26,27</sup>. Unfortunately, during shearing and fibre processing, around one-quarter of short and non-spinnable alpaca fibres are produced as waste and are mainly thrown in a landfill or used in the preparation of low-grade animal feed <sup>28</sup>. To minimize the landfilling and utilizing these valuable fibres, our group have already collected and converted these waste fibres into micron-sized particles in an environmentally friendly manner without altering the proteinaceous functional groups of the parent fibre <sup>28</sup>. We have found that while the fibres were converted into powders, the crystallinity of the powders was decreased and moisture absorption increased <sup>28</sup>.

This current work aims to accelerate the use of textile-based waste materials to reduce the ecological footprint and support the circular economy by using alpaca waste. Here, we have investigated the applicability of alpaca powders wet-spun with polyacrylonitrile (PAN) polymer to enrich the thermal stability and moisture absorption properties of the alpaca/PAN composite fibres. Furthermore, the rheology of the dope solution, morphology, chemical structure, crystallinity and mechanical properties of the wet-spun fibres were examined. To the best of our knowledge, this work represents the first attempt of applying mechanically milled alpaca powders with PAN for the production of alpaca/PAN composite fibres with improved moisture properties and thermal stability. Although there are some reports on the production of bio-based composite fibres with enhanced functional properties, the processes described in those works are not completely free of using chemicals <sup>20,22,24</sup>. Hence, we assume that this study

of adding plain alpaca powder (without any further chemical modification) into the polymeric chain of PAN is a combination of greener and eco-friendly procedure to enrich the functional properties of the composite fibres. Undoubtedly, this research work will lead us to a path of cleaner production of composite fibres due to adopting eco-friendly and sustainable methods.

## **2. Materials and methods**

### *2.1. Materials*

Waste alpaca fibres were provided by Nocturne Alpacas, Buckley, VIC 3240, Australia. Polyacrylonitrile (molecular weight of 150,000 g/mol) was purchased from Sigma-Aldrich. Dimethyl sulfoxide (DMSO) of 99% purity was procured from Merck, Germany. The chemicals were used as received.

### *2.2. Mechanical milling and particle size measurement*

The mechanical milling process of alpaca fibres to convert into powders and their particle size measurement procedure as described before<sup>28</sup>. Briefly, the collected waste alpaca fibres were washed with Eucalyptus wool wash and water (room temperature). After drying overnight at 60 °C in an oven, the fibres were cut into snippets by using a rotary cutter mill (Pulverisette 19 from Fritsch GmbH, Germany). These snippets were converted into a slurry and spray dry powder using Attritor mill (2S, Union Process, USA) and spray dryer (B-290, Buchi Labortechnik AG, Switzerland), respectively. Finally, the spray dried powder was processed through an air jet mill (Sturtevant Inc, USA) to produce the alpaca particles<sup>28</sup>. The distribution of volumetric particle size of the air jet-milled powder was measured where the volume median diameter of 2.5 µm was denoted as d(0.5)<sup>28</sup>. Fig. 1 represents the images of alpaca fibres and particles.



**Fig. 1.** Images of samples: a) alpaca fibres and b) alpaca particles

### *2.3. Preparation of dope solution and rheology measurement*

Control polyacrylonitrile (PAN) dope solution was prepared by adding 18 wt. % of PAN in dimethyl sulfoxide (DMSO) by stirring (65 rpm, 60 °C) for 24 hours to ensure the PAN is completely dissolved. To prepare the alpaca/PAN dope solution, first the alpaca powder was dispersed in DMSO by sonication for 2 hrs, then the PAN polymer was dissolved into DMSO (containing alpaca particles) and stirred overnight at 60 °C. The blending ratio of the alpaca particle and PAN was 10:90, 20:80 and 30:70 at 18 wt. % concentration of the spinning solution. Experiments on higher alpaca content (e.g, 40 %) were also conducted. However, due to the presence of high solid content in the dope solution which resulted in spinneret blocking, hence spinning was not possible. In addition, a range of dope solution concentrations (%) between 12 wt. % and 20 wt. % were trialed. The 18 wt. % concentration was finally found to be the best solution in terms of the viscosity and spinnability. Spinnability is the ability to produce fibres from the polymeric solution even by the use of stirring rod from a beaker<sup>29</sup>. It depends on various factors such as solution viscosity, extrusion ratio and flow rate of the solution.

The corresponding composite alpaca/PAN fibres formed from the alpaca-PAN blends were termed AP (10:90), AP (20:80) and AP (30:70), respectively. A rheometer (The Discovery HR-

3, TA Instruments, USA) was used to determine the viscosity of different dope solutions. The diameter of the geometry was 40 mm with a 2° cone angle and the truncation gap was 49 µm<sup>30-32</sup>. The measurement was performed at 25 °C and the shear rate was between 0.1 and 100 s<sup>-1</sup>. Power-law relationship of the Ostwald de Waele model (Equation 1) was used to express the flow behavior of the dope solutions:

$$\sigma = K\gamma^n \quad (1)$$

where  $\sigma$  is the shear stress in Pascal,  $\gamma$  is the shear rate (1/s), K and n are the consistency index and non-Newtonian index, respectively<sup>33</sup>. The regression parameters of the consistency index (K) and non-Newtonian index (n) were determined by linear curve fitting.

#### 2.4. *Wet spinning of fibres*

The wet spinning of the fibres was carried out using the Dissol (Dissol Pty. Ltd.) wet spinning line fitted with a gear pump and consists of a temperature controlled coagulation bath, a washing zone, a drying zone and a winding zone (Fig. 2). This wet spinning system is capable of spinning up to 1 L of dope solution and 3 kilometres of filament in length at once. The dope solution was extruded through the spinneret (100 µm diameter with 100 holes) at room temperature where a mixture of DMSO and water (60:40) was used as a coagulation medium. After precipitation, the fibres were passed through the washing (ambient temperature) and stretching bath (80 °C) and wound on a spool with a total draw ratio of 4:1.

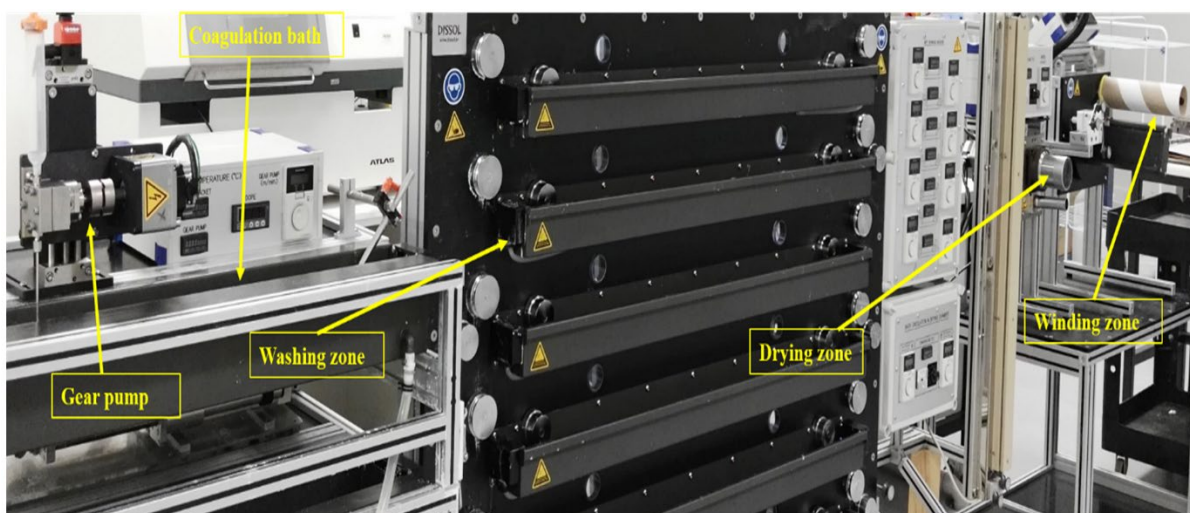


**Fig. 2.** Dissol wet spinning machine

### 2.5. Scanning Electron Microscope (SEM)

The surface and cross-sectional morphologies of the control PAN and alpaca/PAN composite fibres were observed with a Zeiss Supra 55VP scanning electron microscope (SEM), where the accelerating voltage was kept at 3 kV. Leica EM ACE600 gold coater was used to coat fibres prior to imaging.

### 2.6. Fourier-transform infrared spectroscopy (FTIR)

The Fourier-transform infrared (FTIR) spectra analysis of all the fibres was accomplished under Attenuated Total Reflectance (ATR) mode using Vertex 70 (Bruker, Germany) spectrometer with a scan resolution of  $4\text{ cm}^{-1}$  and 32 scans per sample between  $400\text{ cm}^{-1}$  and  $4000\text{ cm}^{-1}$ . Data were collected after baseline correction by OPUS 5.5 software.

### 2.7. Nuclear Magnetic Resonance Spectroscopy (NMR)

The  $^1\text{H}$  NMR and  $^{13}\text{C}$  NMR spectra were recorded on a Bruker spectrometer, Germany. The cross polarisation magic angle spinning (CP-MAS) solid-state  $^{13}\text{C}$  NMR spectra of the samples were recorded on a 300 MHz Bruker Ascend 300 WB spectrometer by using a 4 mm rotor at

spinning rate of 10 KHz and 1600 scans for each sample. Data were extracted using TopSpin 3.2 software.

### *2.8. X-ray diffraction (XRD)*

The crystallinity of the control PAN and composite fibres was analyzed at room temperature by X-ray diffraction (XRD) technique (X'Pert Powder, PANalytical, Netherlands) where the operating voltage and the current flow were 40 kV and 30 mA, respectively. The measurement was taken between 6 to 40°; step size was 0.013° and 250s per step. The crystallinity index (Cr.I.) of the fibres was calculated by Equation (2):

$$\text{Cr.I.} = (I_f - I_s) * 100 / I_f \quad (2)$$

where Cr.I. is the crystallinity index,  $I_f$  is the peak intensity in arbitrary units with 2-theta at 17° and  $I_s$  is the peak intensity in arbitrary units with 2-theta at 28.5°<sup>34</sup>.

### *2.9. Differential Scanning Calorimetry (DSC)*

DSC Q200 (TA Instruments, USA) was used to perform the Differential Scanning Calorimetry (DSC) test. The samples (5 mg) were heated from ambient temperature to 400 °C at a heating rate of 10 °C/min in a nitrogen atmosphere.

### *2.10. Thermogravimetric analysis (TGA)*

To perform the thermogravimetric analysis (TGA) TGA Q50 (TA Instruments, USA) was used where the samples (5 mg) were heated from the ambient temperature to 600 °C at a heating rate of 10 °C/min in a nitrogen atmosphere.

### *2.11. Mechanical testing*

The mechanical properties (tenacity and elongation at break) of the control PAN and the alpaca/PAN composite fibres were determined by Instron 5967, USA. To perform the

mechanical testing, a load cell of 50 N, a gauge length of 100 mm and a crosshead speed of 10 mm/min were adopted. The samples were conditioned for 48 hrs in a standard condition of  $20 \pm 2$  °C and  $62 \pm 2$  % relative humidity prior to the test. The linear density of the fibres was measured in the direct system (tex) which is defined as the mass in grams per 1000 meters of fibre <sup>35</sup>. Each fibre (control PAN and alpaca/PAN) was tested 20 times and the average of the measurements was reported for tenacity (cN/tex) and elongation at break (%) along with the standard deviation.

### *2.12. Moisture properties*

The moisture regain (MR) and moisture content (MC) of the fibre samples were measured in percentage by using ASTM D2495-07 (reapproved 2012) <sup>36,37</sup>. Briefly, around 2 g of each sample was conditioned at standard atmosphere ( $20 \pm 2$  °C and  $62 \pm 2$  % relative humidity) for 48 hrs. The samples were weighed and dried at 110 °C for 4 h in a laboratory conventional oven. The samples were then reweighed and the moisture regain and moisture content were calculated according to the Equation (3) and Equation (4), respectively:

$$\text{MR (\%)} = (M-D) / D * 100 \quad (3)$$

$$\text{MC (\%)} = (M-D) / M * 100 \quad (4)$$

where, M is the weight of the conditioned sample and D is the weight of the oven-dried sample. Every sample was tested five times and the average was reported.

### 3. Results and discussion

#### 3.1. Rheology, morphology and mechanical properties

##### 3.1.1. Rheological properties

The rheology of the dope solutions is presented in Fig. 3(a). It can be seen that the control PAN had the highest viscosity among all the dope solutions and the viscosity reduced continuously with the addition of alpaca particles<sup>30</sup>. Furthermore, at an elevated shear rate, the viscosity of all the solutions decreased, which confirmed the shear thinning (non-Newtonian) behavior<sup>30,31</sup>. It has been reported that in a polymeric solution when the shear rate is low the breakage rate of the large molecular entanglements is encountered by the formation of new molecular entanglements<sup>32</sup>. However, during a higher shear rate, the balance of this molecular reconstruction is hindered and the interfaces between the molecules declines resulting in lower viscosity of the solution<sup>32,38</sup>. Since the solutions displayed shear thinning behavior, to evaluate the spinnability of the dope solutions, the non-Newtonian index was calculated<sup>33</sup>. The logarithmic curves of shear stress and shear rate are shown in Fig. 3(b) and the consistency index (K), non-Newtonian index (n), and correlation coefficient ( $R^2$ ) are shown in Table 1. The spinnability of the control PAN dope solution (n= 0.66) was higher than that of alpaca/PAN dope solutions and with the increase of alpaca content the spinnability reduced, as the higher the value of n, the more the spinnability of the dope solutions<sup>33</sup>. The alpaca particles were dispersed into the dope solution rather than complete dissolution. This could be the reason for the reduction in viscosity and non-Newtonian index (n). A similar result of reduced viscosity was found when lignin was added to PAN polymer in preparation of lignin/PAN dope solution<sup>30,31</sup>.

**Table 1**

The value of  $K$ ,  $n$ , and  $R^2$  after fitting the logarithmic curves of shear stress and shear rate

Sample	Consistency index (k)	Non-Newtonian index (n)	Correlation coefficient ( $R^2$ )
Control PAN	2.07	0.66	0.99
AP (10:90)	2.04	0.65	0.99
AP (20:80)	2.14	0.59	0.99
AP (30:70)	2.14	0.58	0.99

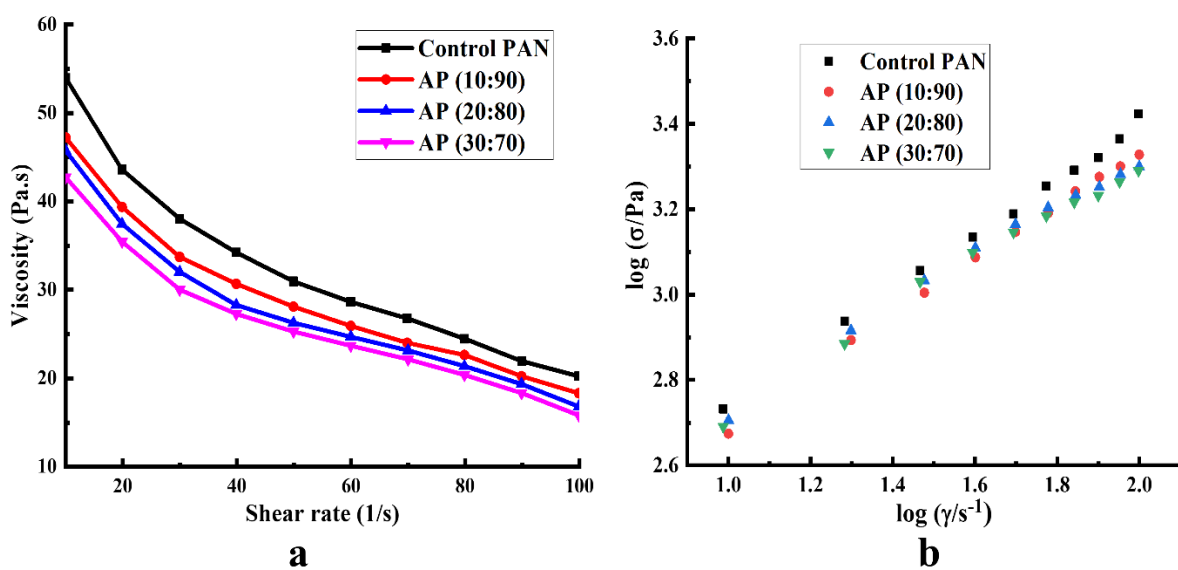


**Fig. 3.** Viscosity versus shear rate (a) and logarithmic plots of shear stress vs shear rate (b) of 18 wt. % control PAN and alpaca/PAN dope solutions

### 3.1.2. Morphological analysis

The longitudinal and cross-sectional SEM images of control PAN and alpaca/PAN composite fibres with different alpaca percentages are presented in Fig. 4. Control PAN fibres showed a ribbon-like appearance with a smooth fibre surface, which might be the result of using DMSO and water as the precipitation bath that led to probable sulfonation of DMSO<sup>39</sup>. A similar effect on the surface of PAN was also reported by Kruchinin et al. where different combinations of coagulation bath were trialled but only the DMSO: water bath provided a smooth surface of PAN due to the sulfonation<sup>39</sup>. In addition, the cross-sectional image of the control PAN fibres

showed a typical bean shape that might be due to the counter-diffusion mechanism of the solvent (out) and non-solvent (in) into the coagulation bath <sup>30</sup>. Unexpectedly, the fibres exhibited one large (micron-sized) and many tiny (nano-sized) pores in the cross-section that could be as the result of a lower draw ratio of the fibres during the spinning process (Fig. 4).

When the alpaca particle was added to the PAN solution at 10 %, 20 %, and 30 % weight ratios, the composite fibres exhibited almost circular cross-sectional shape having striations and non-smooth fibre surface with porous and void areas. As the alpaca particles were dispersed into the solvent rather than complete dissolution, it might be possible that during stretching of fibres from the coagulation bath to the winding spool, the striations are formed and appeared on the fibre surface.

It is known that the moisture transfer properties of alpaca fibres are higher than the acrylic fibres and has a contribution to the comfort properties <sup>35</sup>. However, the acrylic fibres have poor moisture transfer properties <sup>10,11,35</sup>. Thus, the change in morphology of the PAN by addition of the alpaca may increase the moisture transfer properties of the acrylic fibres. We believe that both the voids and striations of the composite fibres could be able to enhance the moisture regain of the fibres which is discussed later.

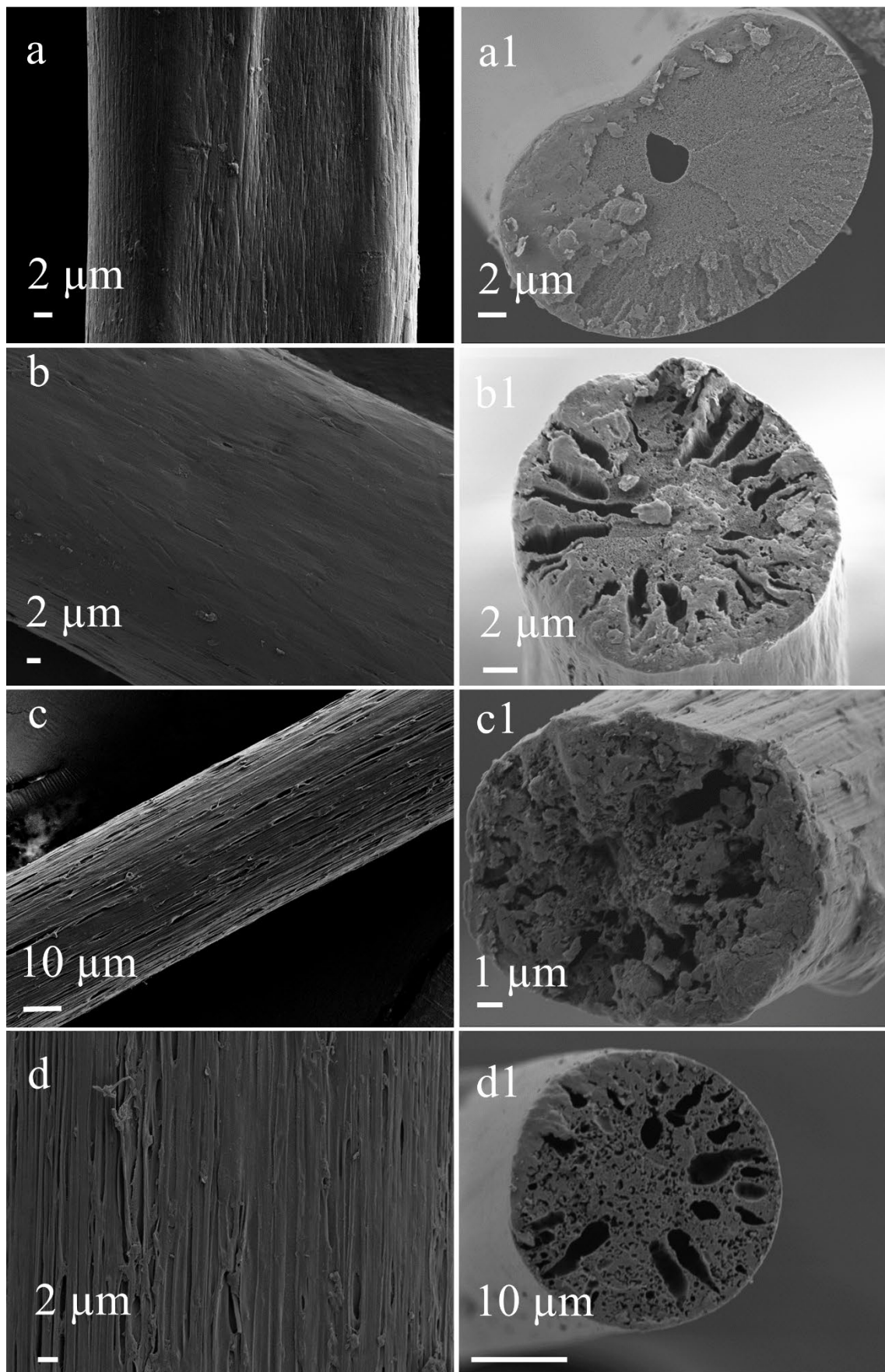


**Fig. 4.** Longitudinal and cross-sectional SEM images: a-a1) control PAN, b-b1) alpaca/PAN (10:90), c-c1) alpaca/PAN (20:80) and d-d1) alpaca/PAN (30:70)

### *3.1.3. Mechanical properties*

The load-elongation curve and the average values of fibre diameter ( $\mu\text{m}$ ), linear density (tex), tenacity (cN/tex) and elongation at break (%) of all the fibres are shown in Fig. 5 and Table 2, respectively. A relatively large fibre diameter ranging from around 30  $\mu\text{m}$  to 50  $\mu\text{m}$  was found in all the fibres and the linear density was approximately between 29 tex and 34 tex. This might be due to the lower drawing ratio during the wet spinning (draw ratio 4). The tenacity of the control PAN fibre spun in this study was 11.4 cN/tex. Similarly, the tenacity of the composite fibres was reduced by approximately 4 % for AP (10:90), 31 % for AP (20:80) and 41 % for AP (30:70) than that of pure PAN fibre with the addition of alpaca particles. The elongation at break of the composite fibres reduced by around 25 % for AP (10:90), 27 % for AP (20:80) and 29 % for AP (30:70) than that of the control PAN. The reason for the deterioration of the mechanical properties of the composite fibres might be due to the increased number of void formations (Fig. 4) and higher fibre diameter (Table 2). The presence of the voids on the surface and inner side of the fibre structure results in stress concentration when the tensile force is applied. This leads to a decrease in tenacity and finally the fibre breaks. The larger diameter of all the fibres could be another reason for the lower mechanical properties<sup>40</sup>. Further investigations on the modification of various wet spinning parameters to wet spin the alpaca/PAN composite fibres with reduced fibre diameter and enhanced mechanical properties are currently being examined.

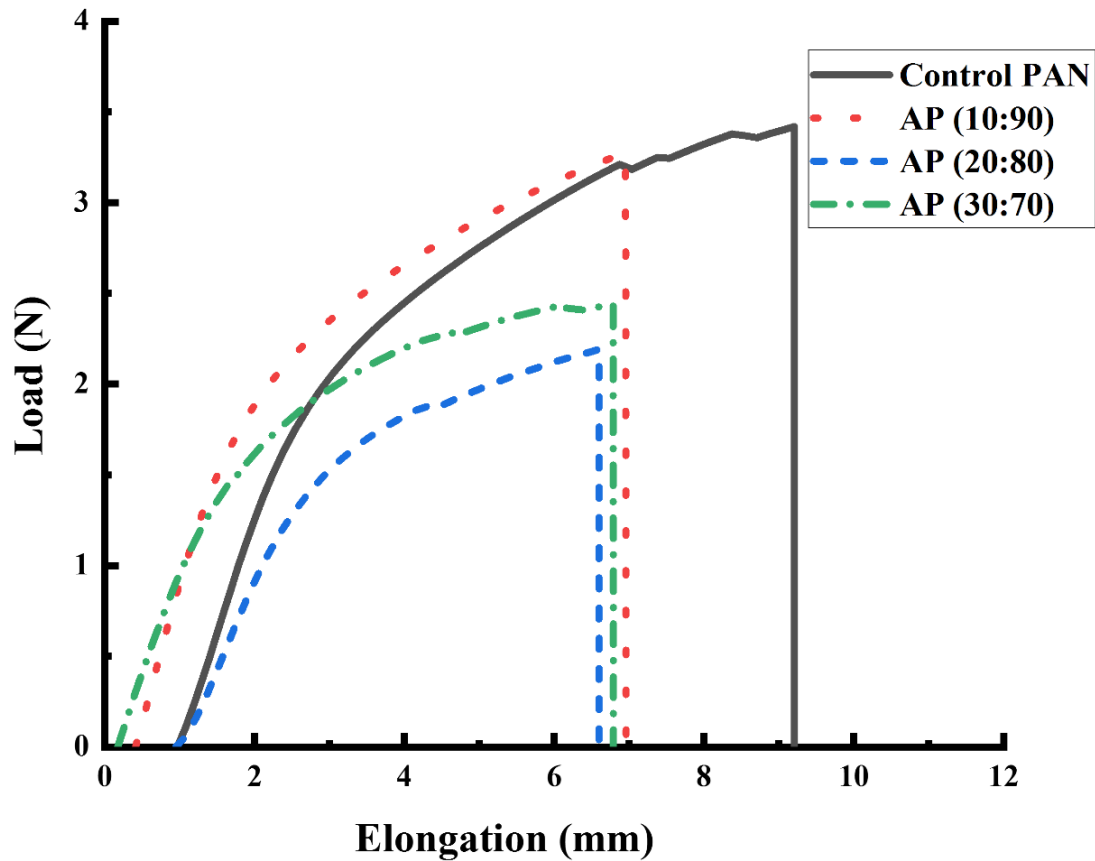


Fig. 5. The load-elongation curve of control PAN and the alpaca/PAN composite fibres

Table 2

Mechanical properties of control PAN and alpaca/PAN composite fibres

Sample	Diameter ( $\mu\text{m}$ )	Linear density (tex)	Tenacity (cN/tex)	Elongation at break (%)
Control PAN	$34.67 \pm 2.44$	$29.16 \pm 1.14$	$11.4 \pm 0.20$	$9.21 \pm 0.14$
AP (10:90)	$30.78 \pm 2.29$	$28.27 \pm 1.23$	$10.94 \pm 0.31$	$6.95 \pm 0.21$
AP (20:80)	$32.44 \pm 2.37$	$31.14 \pm 1.82$	$7.84 \pm 0.38$	$6.79 \pm 0.26$
AP (30:70)	$47.83 \pm 2.77$	$33.35 \pm 1.18$	$6.64 \pm 0.26$	$6.59 \pm 0.26$

### 3.2. Chemical structural analysis

The chemical structures of all the fibre samples were determined by Fourier-transform infrared spectroscopy (FTIR) and Nuclear Magnetic Resonance (NMR) techniques, as shown in Fig. 6 and 7, respectively. The protein structures of alpaca particles are primarily identified by the

presence of amide A, amide I, amide II and amide III bands. The strong and broad absorption peak at around  $3300\text{ cm}^{-1}$  represents the presence of both N-H stretching (amide A) and O-H stretching. The strong absorption peaks at  $1540\text{ cm}^{-1}$  and  $1650\text{ cm}^{-1}$  are attributed to the methyl C-H deformation and C=O stretching that represent the amide II and amide I, respectively. The components of amide I band frequencies are very closely interrelated with the other secondary elements of proteins and it is the result of almost 80% of C=O stretching of the peptide linkage whereas the amide II band is reflecting lower conformational sensitivity of proteins, which is primarily obtained from CN stretching vibration and NH bending<sup>41</sup>. In addition, the other weak band at  $1240\text{ cm}^{-1}$  stands for the C-N and C-O stretching vibrations (amide III)<sup>42,43</sup>. The other two prominent peaks are at  $2850\text{ cm}^{-1}$  and  $2930\text{ cm}^{-1}$ , representing the symmetric and asymmetric C-H stretching vibrations of methylene group, respectively<sup>44</sup>. The control PAN fibre represented its main characteristic peak at  $2240\text{ cm}^{-1}$  assigned to the C≡N (nitrile group) and the other peaks at  $1470\text{ cm}^{-1}$  and  $2930\text{ cm}^{-1}$  ascribed to the bending and stretching vibration of methylene groups, respectively<sup>30</sup>. Nitrile group is composed of one sigma ( $\sigma$ ) bond and two pi ( $\pi$ ) bonds that makes it stronger in nature. In composite fibres, all the characteristic peaks of both alpaca and PAN were observed with no further new absorption peaks. This might be due to the fact that while the alpaca powder dispersed into the PAN system it was not able to break the strong  $\sigma$  and  $\pi$  bonds to create new chemical bonds. Hence, these results recommend the proper blending of alpaca and PAN in the dope solution by avoiding any major chemical changes or deformations, which was also found in the previous works<sup>30,31</sup>.

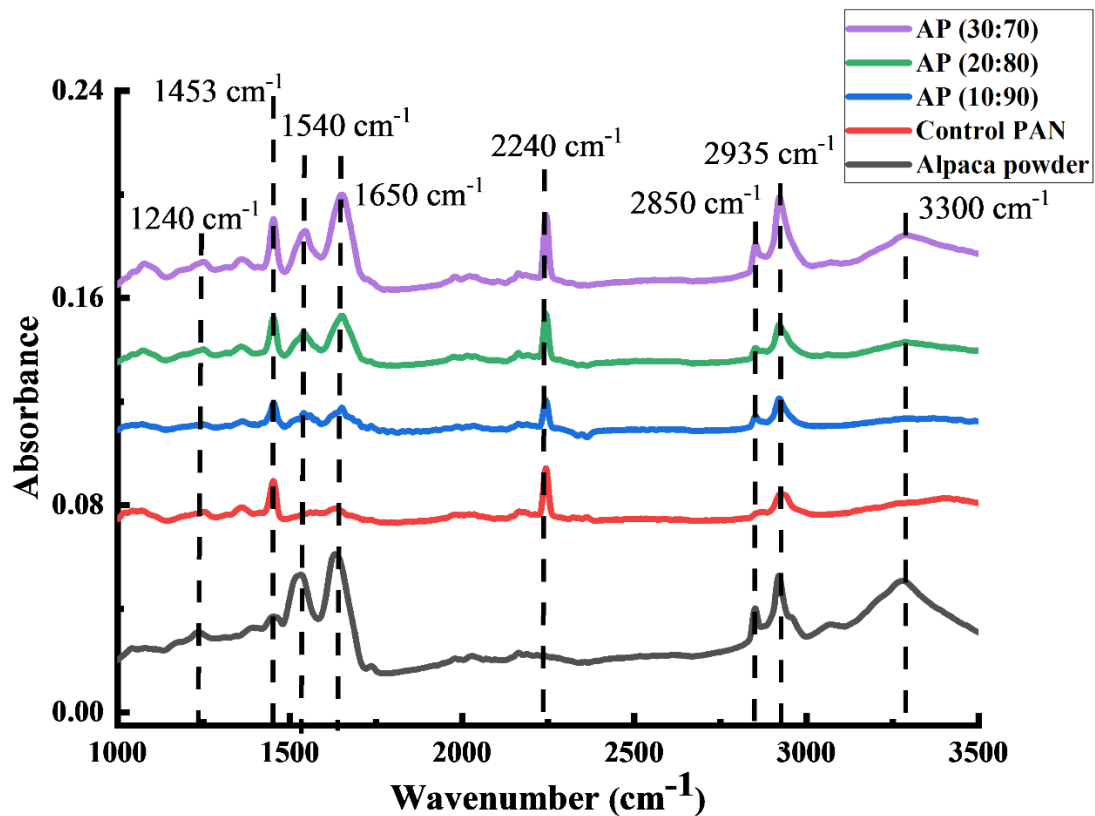


**Fig. 6.** FTIR analysis of alpaca powder, control PAN, and alpaca/PAN composite fibres

On the other hand, from the solid-state <sup>13</sup>C CP-MAS NMR (Fig. 7), it is evident that the alpaca particle showed the typical carbonyl carbon (C=O) peak at 174 ppm<sup>33</sup>. The control PAN fibre exhibited its characteristic methane carbon (CH), methylene carbon (CH<sub>2</sub>) and nitrile carbon (CN) peaks at 28-29, 36-37 and 120-121 ppm, respectively<sup>45</sup>. From Fig. 7 it can be seen that the alpaca/PAN composite fibres represent the corresponding peaks of both protein and PAN polymer. In addition, no new or additional peak was found in the NMR analysis of the composite fibres, which confirms the proper mixing of the polymers in the dope solution and further supports the findings of the FTIR analysis (Fig. 6).

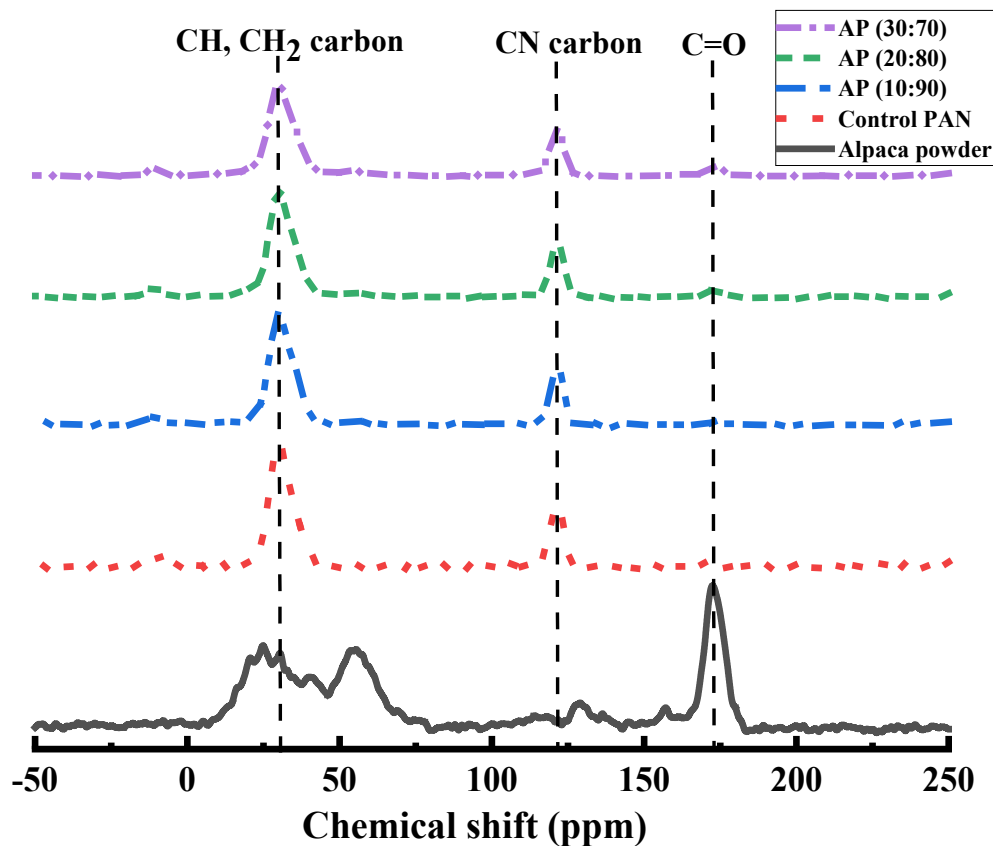


**Fig. 7.** NMR spectroscopy of alpaca powder, control PAN, and alpaca/PAN composite fibres

### 3.3 Thermal properties of the fibres

The DSC and TGA analysis of control PAN and alpaca/PAN composite fibres are shown in Fig. 8 (a & b). All the fibres showed only one glass transition temperature ( $T_g$ ) between  $60\text{ }^{\circ}\text{C}$  and  $80\text{ }^{\circ}\text{C}$  that ultimately resembles the proper miscibility of alpaca powder and PAN polymer with no phase separation during the formation of fibre<sup>31,46</sup>. An exothermic peak between  $290\text{ }^{\circ}\text{C}$  and  $296\text{ }^{\circ}\text{C}$  was evident from Fig. 8(a) that corresponds to the wet-spun control PAN fibres. However, the decomposition temperature of the composite fibre with only 10 % alpaca, moved to around  $310\text{ }^{\circ}\text{C}$ . This tendency might be due to the proper dispersion and physical bonding of alpaca powder into the PAN system, as previously it was found that the mechanically milled alpaca powder possess higher decomposition temperature rather than the alpaca fibres<sup>28</sup>. In addition, the polypeptide chains of the protein structure have tied up the flexible chain of PAN

that restricts the easy movement of PAN<sup>46</sup>. Therefore, this phenomenon led to the increment of the decomposition temperature of the alpaca/PAN composite fibres.

Thermal degradation is an important property of polymeric materials that is determined at higher temperatures. The thermal degradation of the control PAN and alpaca/PAN composite fibres is shown in Fig. 8(b). The major decomposition temperature was evident at around 286 °C in the case of control PAN fibres where the nitrile (C-N) bonds degrade<sup>31,47</sup>. In addition, the second decomposition occurred at approximately 430 °C that belongs to the breakage of C-C bonds<sup>47</sup>. For composite fibres, it was found that the addition of only 10 % alpaca powder to the PAN polymeric chain increased the thermal degradation temperature from almost 286 °C to 305 °C, which agrees with the study where the addition of lignin increased the degradation temperature of the lignin/PAN fibres<sup>31</sup>. Similarly, the addition of 30 % alpaca enhanced the degradation temperature up to 320 °C, which might be due to the protein structure of the alpaca powder and large amounts of powder in the dope solution. This increment in decomposition temperature with the addition of alpaca to PAN polymer ensures the increased thermal stability of the alpaca/PAN composite fibres than that of pure PAN fibres, which is also supported by the DSC analysis (Fig. 8a).

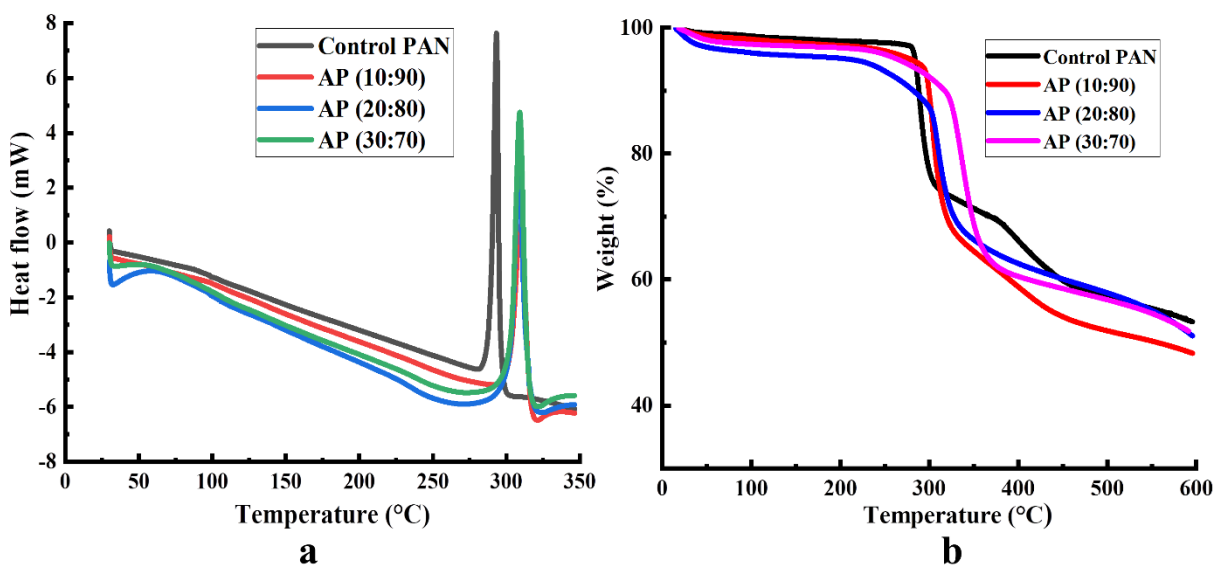


**Fig. 8.** Thermal analysis of control PAN and alpaca/PAN composite fibres (a) DSC & (b) TGA

### *3.4. Crystallinity and moisture properties*

#### *3.4.1. Crystallinity of the fibres*

The diffraction patterns of control PAN and alpaca/PAN composite fibres are shown in Fig. 9. The calculated crystallinity index (Cr.I.) of all the fibres are tabulated in Table 3. The diffraction pattern of control PAN fibre showed a characteristic broad halo  $2\theta$  peak at  $17^\circ$  of the crystalline spacing of  $5.2 \text{ \AA}$  and another small intensity  $2\theta$  peak at  $28.5^\circ$  indicating the crystalline spacing of  $3.1 \text{ \AA}$ <sup>48</sup>. In a diffraction pattern, the halo-peaks are due to the higher crystalline region whereas the broader peaks represent the lower crystalline or higher amorphous region<sup>40</sup>. From Table 3, it can be found that the control PAN fibres showed around 55 % crystallinity whereas it was gradually reduced with the increment of alpaca content in the composite fibres. As the broadness of the peak at  $17^\circ$  of the composite fibres increased (Fig. 9), the crystallinity of the composite fibres decreased (Table 3). The results are supporting literature where the lignin/PAN composite fibres exhibited lower crystallinity compared to pure PAN-based carbon fibres when the diffraction peaks of the composite fibres were broadened and less pronounced<sup>30</sup>. Hence, it is expected that the moisture absorption properties of the composite fibres would be enhanced because of the increased amorphous region.

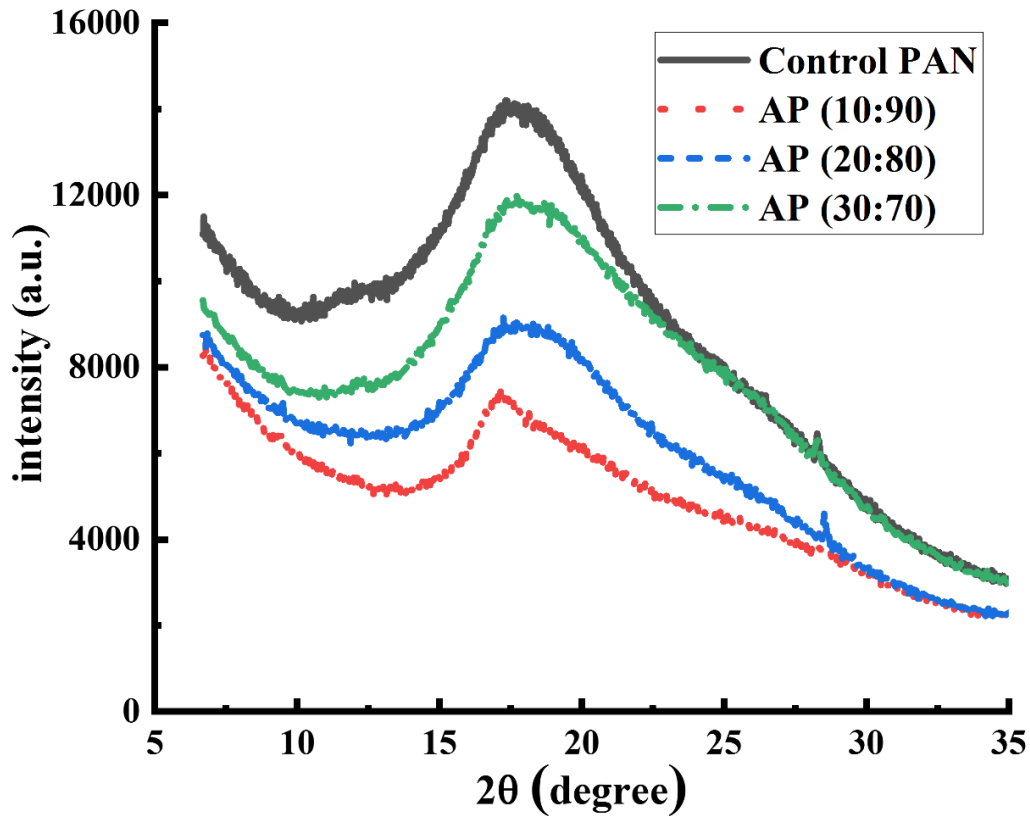


**Fig. 9.** XRD analysis of control PAN and alpaca/PAN composite fibres

**Table 3**

Crystallinity index of control PAN and alpaca/PAN composite fibres

Sample	Peak intensity at $17^{\circ}$ ( $I_f$ )	Peak intensity at $28.5^{\circ}$ ( $I_s$ )	Crystallinity index (%)
Control PAN	14193.09	6455.41	54.51
AP (10:90)	7503.65	3820.75	49.08
AP (20:80)	9156.87	4955.32	45.88
AP (30:70)	11991.03	6981.08	41.78

### 3.4.2. Moisture properties analysis

The moisture regain (%) and moisture content (%) of all the fibres are shown in Fig. 10. It was apparent that with the incorporation of alpaca, the moisture properties of the composite fibres increased. Unlike natural fibres, synthetic fibres have low moisture properties. However, it is

well known that higher regain of fibre can enhance the next to skin comfort of the wearer <sup>49</sup>. While the moisture regain of alpaca fibre ranges from 14 % to 16 %, the moisture regain of acrylic fibres ranges between 1.5 % and 2.5 % <sup>11,35</sup>. In this work, the moisture regain and moisture content of the acrylic fibre were found to be 2.42 % and 2.36 %, respectively. However, when the alpaca particle was added to PAN, the composite fibres showed increased moisture regain and moisture content values than that of the control PAN fibres. It was found that with the addition of 10 % alpaca, the moisture regain and moisture content were increased to around 60 % compared to the control PAN fibre. The moisture regain and moisture content were more than three times greater than the pure PAN, respectively with the addition of 30 % alpaca than that of pure acrylic fibres. While naturally, alpaca fibres are more moisture absorbent <sup>35</sup> the FTIR analysis (Fig. 6) showed that alpaca possesses a strong and broad -OH group that is responsible for the higher moisture absorption. In addition, the formation of porous and void areas on the surface and cross-section of the fibres as observed by SEM images (Fig. 4), could also be accountable for the enhancement of the moisture properties of the composite fibres. Furthermore, the reduced crystalline area (Fig. 9 & Table 3) in the composite fibres is also responsible for the increment of moisture regain (%) than that of pure PAN fibres

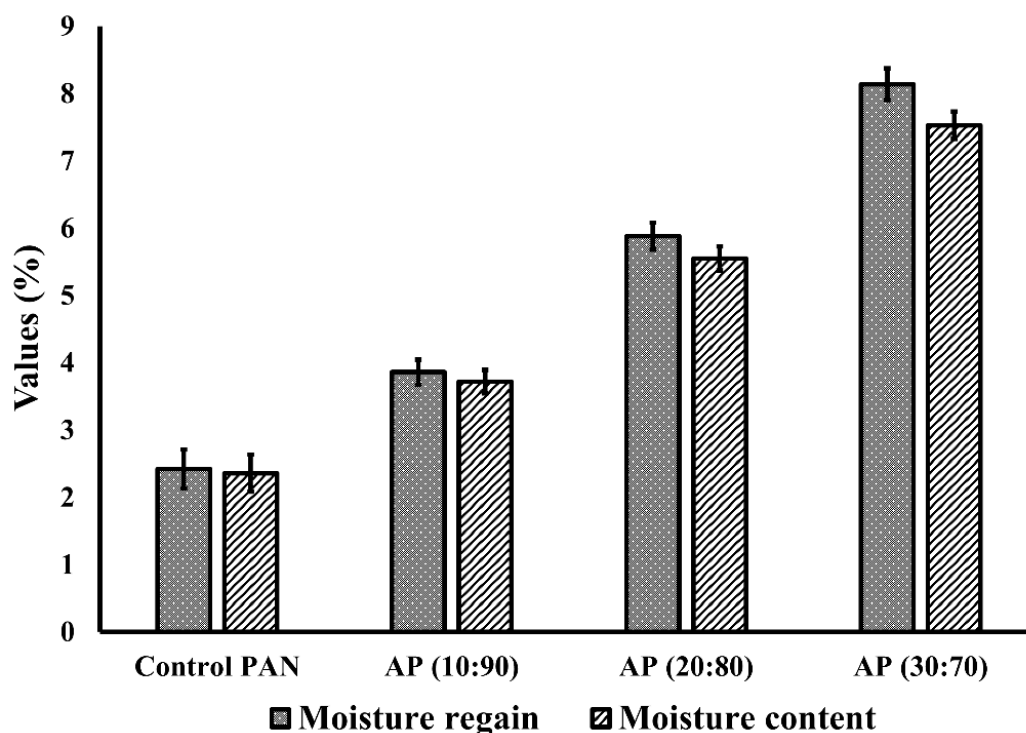


**Fig. 10.** Moisture regain (%) and content (%) of control PAN and alpaca/PAN composite fibres

#### 4. Conclusion

In our work, we have tried to use the eco-friendly and sustainable procedures to convert the non-spinnable waste alpaca fibres into powders. Thereafter, these powders were blended with PAN polymer to wet spin the alpaca/PAN composite fibres with improved thermal and moisture properties for their future application. The SEM images of the control PAN fibres exhibited smooth fibre surface with typical ribbon-like shape whereas the composite fibres showed striations on the fibre surface with inner porous and void areas. The tenacity and elongation at break of the composite fibres decreased with an increasing amount of alpaca powders applied to the dope solution. No new absorption peaks appeared in the composite fibres other than the characteristics of protein and nitrile peaks through FTIR and NMR studies that ultimately confirms the proper blending and mixing between two polymers. From the DSC and TGA analyses, we have found that by adding alpaca powders the decomposition

temperature was raised which confirms the increment of thermal stability of the composite fibres. It was also found that the crystallinity of the composite fibres reduced compared to the control PAN fibres with the increased alpaca content. Furthermore, with the addition of alpaca powders, the moisture properties of the composite fibres increased more than three times than that of the control PAN. The improved moisture regains of acrylic fibres resulting from the addition of alpaca will facilitate the use of acrylic fibres in a wide range of possible applications. From these observations, we can conclude that this work ensures the ecological reuse of textile waste materials and manufacturing of composite fibres with enhanced thermal and moisture properties while loading alpaca with the PAN polymer reduces the proportion of synthetic PAN in the dope solution.

## **Acknowledgment**

The current study was supported by Deakin University Postgraduate Research Scholarship (DUPRS) and Lincoln Agritech Ltd awarded to the first author and was carried out with the support of the Deakin Advanced Characterization Facility. The authors acknowledge the Australian Research Council (FT130100380, IH140100018, and DP170102859) and the Australian National Fabrication Facility (ANFF) for access to fiber fabrication and analysis facilities (Deakin). Mr Abu Naser Md Ahsanul Haque is acknowledged for his comments on early version of the manuscripts.

## **References**

1. Alam, M. S.; Selvanathan, E.; Selvanathan, S.; Hossain, M., *Review of Development Economics*. 2019, 23, 454-474.
2. Kumar, P. S.; Pavithra, K. G. In *Water in Textiles and Fashion*; Elsevier, 2019.
3. Karbownik, I.; Fiedot, M.; Rac, O.; Suchorska-Woźniak, P.; Rybicki, T.; Teterycz, H., *Polymer*. 2015, 75, 97-108.
4. Senokos, E.; Ou, Y.; Torres, J. J.; Sket, F.; González, C.; Marcilla, R.; Vilatela, J. J., *Scientific reports*. 2018, 8, 3407.

5. Gurunathan, T.; Mohanty, S.; Nayak, S. K., *Composites Part A: Applied Science and Manufacturing*. 2015, 77, 1-25.
6. Chien, A.-T.; Gulgunje, P. V.; Chae, H. G.; Joshi, A. S.; Moon, J.; Feng, B.; Peterson, G. P.; Kumar, S., *Polymer*. 2013, 54, 6210-6217.
7. Kim, N. K.; Lin, R. J. T.; Bhattacharyya, D., *Composites Part A: Applied Science and Manufacturing*. 2017, 100, 215-226.
8. Rizvi, A.; Andalib, Z. K.; Park, C. B., *Polymer*. 2017, 110, 139-148.
9. Reifler, F. A.; Hufenus, R.; Krehel, M.; Zraggen, E.; Rossi, R. M.; Scherer, L. J., *Polymer*. 2014, 55, 5695-5707.
10. McIntyre, J. E., *Synthetic fibres: nylon, polyester, acrylic, polyolefin*; Taylor & Francis US, 2005.
11. Masson, J., *Acrylic fiber technology and applications*; CRC Press, 1995.
12. Madakbaş, S.; Çakmakçı, E.; Kahraman, M. V., *Thermochimica Acta*. 2013, 552, 1-4.
13. Kaur, J.; Millington, K.; Smith, S., *Journal of Applied Polymer Science*. 2016, 133, 43963.
14. Sabantina, L.; Klöcker, M.; Wortmann, M.; Mirasol, J. R.; Cordero, T.; Moritzer, E.; Finsterbusch, K.; Ehrmann, A., *Journal of Industrial Textiles*. 2019, 1-16.
15. Bajaj, P.; Sreekumar, T.; Sen, K., *Journal of applied polymer science*. 2002, 86, 773-787.
16. Bahrami, S.; Bajaj, P.; Sen, K., *Journal of applied polymer science*. 2003, 89, 1825-1837.
17. Dong, X. G.; Wang, C. G.; Bai, Y. J.; Cao, W. W., *Journal of applied polymer science*. 2007, 105, 1221-1227.
18. Liu, Y.-C.; Xiong, Y.; Lu, D.-N., *Applied surface science*. 2006, 252, 2960-2966.
19. Bajaj, P.; Paliwal, D. K., *Indian Journal of Fibre & Textile Research*. 1991, 16, 89-99.
20. Ahmad Rasyid, M.; Salim, M.; Akil, H.; Karger-Kocsis, J., *Express Polymer Letters*. 2019, 13, 553-564.
21. Xu, J.; Tian, C.; Ma, Z.; Gao, M.; Guo, H.; Yao, Z., *Journal of thermal analysis and calorimetry*. 2000, 63, 501-506.
22. Wan, Y.; Luo, H.; He, F.; Liang, H.; Huang, Y.; Li, X., *Composites Science and Technology*. 2009, 69, 1212-1217.
23. Soroudi, A.; Jakubowicz, I., *European Polymer Journal*. 2013, 49, 2839-2858.

24. Siakeng, R.; Jawaid, M.; Ariffin, H.; Sapuan, S.; Asim, M.; Saba, N., *Polymer Composites*. 2019, 40, 446-463.
25. Fan, R.; Yang, G.; Dong, C., *Asian-Australasian Journal of Animal Sciences*. 2010, 23, 444-449.
26. Aluigi, A.; Tonetti, C.; Rombaldoni, F.; Puglia, D.; Fortunati, E.; Armentano, I.; Santulli, C.; Torre, L.; Kenny, J. M., *Journal of materials science*. 2014, 49, 6257-6269.
27. Fan, J.; Lau, L. In *Engineering Apparel Fabrics and Garments*; Fan, J.; Hunter, L., Eds.; Woodhead Publishing Limited: Oxford, 2009.
28. Al Faruque, M. A.; Remadevi, R.; Wang, X.; Naebe, M., *Powder Technology*. 2019, 342, 848-855.
29. Paul, D., *Journal of Applied Polymer Science*. 1968, 12, 2273-2298.
30. Jin, J.; Ogale, A. A., *Journal of Applied Polymer Science*. 2018, 135, 1-9.
31. Oroumei, A.; Fox, B.; Naebe, M., *ACS Sustainable Chemistry & Engineering*. 2015, 3, 758-769.
32. Aluigi, A.; Vineis, C.; Varesano, A.; Mazzuchetti, G.; Ferrero, F.; Tonin, C., *European Polymer Journal*. 2008, 44, 2465-2475.
33. Zheng, S.; Nie, Y.; Zhang, S.; Zhang, X.; Wang, L., *ACS Sustainable Chemistry & Engineering*. 2015, 3, 2925-2932.
34. El-Zaher, N., *Polymer-plastics technology and engineering*. 2001, 40, 689-702.
35. Broadbent, A. D., *Basic principles of textile coloration*; Society of Dyers and Colourists: West Yorkshire, England, 2001.
36. ASTM. American Society for Testing and Materials, USA: 2012.
37. Remadevi, R.; Gordon, S.; Wang, X.; Rajkhowa, R., *Textile Research Journal*. 2017, 87, 2204-2213.
38. Mezger, T. G., *The rheology handbook: for users of rotational and oscillatory rheometers*; Vincentz Network GmbH & Co KG: Hannover, Germany, 2006.
39. Kruchinin, N.; Spirova, T.; Medvedev, V.; Serkov, A.; Radishevskii, M.; Volodin, V.; Prokhorov, V.; Krutova, I.; Egorova, R.; Grekhova, E., *Fibre Chemistry*. 1992, 23, 169-174.
40. Morris, E. A.; Weisenberger, M. C.; Rice, G. W., *Fibers*. 2015, 3, 560-574.
41. Kong, J.; Yu, S., *Acta biochimica et biophysica Sinica*. 2007, 39, 549-559.
42. Li, R.; Wang, D., *Journal of Applied Polymer Science*. 2013, 127, 2648-2653.
43. Aluigi, A.; Zoccola, M.; Vineis, C.; Tonin, C.; Ferrero, F.; Canetti, M., *International Journal of Biological Macromolecules*. 2007, 41, 266-273.
44. Hsu, J.-H.; Lo, S.-L., *Environmental Pollution*. 1999, 104, 189-196.

45. Kamide, K.; Yamazaki, H.; Okajima, K.; Hikichi, K., *Polymer journal*. 1985, 17, 1233.
46. Mousavioun, P.; Halley, P. J.; Doherty, W. O. S., *Industrial Crops and Products*. 2013, 50, 270-275.
47. Seydibeyoğlu, M. Ö., *Journal of Biomedicine and Biotechnology*. 2012, 2012, 1-8.
48. Lee, S.; Kim, J.; Ku, B.-C.; Kim, J.; Joh, H.-I., *Advances in chemical engineering and science*. 2012, 2, 275.
49. Woodings, C., *Regenerated cellulose fibres*; Woodhead Publishing Limited: England, 2001.
50. Howsmon, J. A., *Textile Research Journal*. 1949, 19, 152-162.